Electronic Supplementary Material (ESI) for Physical Chemistry Chemical Physics.

Electronic Supplementary Information

for

Molecular rotators anchored on rod-like anionic coordination polymer adhered by charge-assisted hydrogen bond

Hui Xiao,[a] Wei-Yu Hu,[a] Qing Wang,[b] Cheng-Hui Zeng,[a] Hao-Hong Li,[c] Haiming Liu,[b] Zi-Yi Du[a,*] and Chun-Ting He[a]

[a]*College of Chemistry and Chemical Engineering, Jiangxi Normal University, Nanchang 330022, China*

[b]*School of Physical Science and Technology, ShanghaiTech University, Shanghai 201210, China*

[c]*College of Chemistry, Fuzhou University, Fuzhou 350108, China*

**Correspondence to: Zi-Yi Du, E-mail: ziyidu@gmail.com*

Table S1 Summary of crystal data and structural refinements for **1** at different temperatures

Empirical formula	$C_5H_{14}NBr_3Cd$ (FW = 440.30)					
Temperature (K)	173(2)	203(2)	233(2)	273(2)	293(2)	313(2)
Space group	$P2_1/n$					
a (Å)	7.5549(2)	7.5782(2)	7.6022(3)	7.6240(3)	7.6369(3)	7.6486(4)
b (Å)	16.4113(6)	16.4426(6)	16.4869(7)	16.5760(8)	16.6462(8)	16.7161(1)
c (Å)	9.6428(3)	9.6674(3)	9.6894(4)	9.7148(4)	9.7245(4)	9.7365(5)
V/Å^3	1176.06(7)	1184.39(7)	1193.67(9)	1206.82(9)	1215.46(9)	1224.93(1)
Z	4					
D_{calcd}/g cm^{-3}	2.487	2.469	2.450	2.423	2.406	2.388
μ/mm^{-1}	11.995	11.910	11.818	11.689	11.606	11.516
GOF on F^2	1.052	1.066	1.045	1.059	1.061	1.043
R_1, wR_2 [$I > 2\sigma(I)$][a]	0.0288, 0.0615	0.0304, 0.0654	0.0384, 0.0850	0.0378, 0.0855	0.0419, 0.0947	0.0493, 0.1417
R_1, wR_2 (all data)	0.0374, 0.0636	0.0500, 0.0690	0.0556, 0.0895	0.0669, 0.0938	0.0655, 0.1018	0.0835, 0.1589
Refined content for N1-containing cation[b]	1.000	0.824	0.747	0.688	0.645	0.632

[a] $R_1 = \sum||F_o| - |F_c||/\sum|F_o|$, $wR_2 = \{\sum w[(F_o)^2 - (F_c)^2]^2/\sum w[(F_o)^2]^2\}^{1/2}$

[b] The N1/N1'-containing $(i\text{-PrNHMe}_2)^+$ cation displays two-fold disordered during the structural refinement.

Table S2 Selected bond lengths (Å) for **1** at different temperatures

173 K			
Cd1–Br1	2.5989(4)	Cd1–Br2	2.6076(5)
Cd1–Br3	2.5758(4)	Cd1–Br1#1	2.9696(5)
Cd1–Br2#2	2.8773(4)		
203 K			
Cd1–Br1	2.5971(5)	Cd1–Br2	2.6056(5)
Cd1–Br3	2.5770(5)	Cd1–Br1#1	2.9728(5)
Cd1–Br2#3	2.8854(5)		
233 K			
Cd1–Br1	2.5961(6)	Cd1–Br2	2.6036(6)
Cd1–Br3	2.5754(6)	Cd1–Br1#1	2.9772(6)
Cd1–Br2#3	2.8950(6)		
273 K			
Cd1–Br1	2.5938(6)	Cd1–Br2	2.6011(6)
Cd1–Br3	2.5755(6)	Cd1–Br1#1	2.9806(7)
Cd1–Br2#3	2.9084(6)		
293 K			
Cd1–Br1	2.5928(7)	Cd1–Br2	2.6000(7)
Cd1–Br3	2.5732(7)	Cd1–Br1#1	2.9851(8)
Cd1–Br2#3	2.9159(7)		
313 K			
Cd1–Br1	2.591(1)	Cd1–Br2	2.5951(9)
Cd1–Br3	2.572(1)	Cd1–Br1#1	2.987(1)
Cd1–Br2#3	2.9269(9)		

Symmetry codes: #1. 1 − *x*, 1 − *y*, 1 − *z*; #2. −*x*, 1 − *y*, 1 − *z*; #3. 2 − *x*, 1 − *y*, 1 − *z*.

Table S3 The hydrogen-bond geometries (Å, °) for **1** at different temperatures

	D–H···A	D–H	H···A	D···A	Angle
173 K	N1–H1···Br3	0.9999(3)	2.4619(4)	3.3572(3)	148.8(2)
203 K	N1–H1···Br3	0.9802(5)	2.4744(4)	3.3509(6)	148.7(3)
	N1'–H1'···Br3	0.9793(3)	2.4231(4)	2.3324(3)	154.3(1)
233 K	N1–H1···Br3	0.9803(7)	2.4601(4)	3.3440(8)	149.8(4)
	N1'–H1'···Br3	0.9822(2)	2.4222(4)	3.3252(2)	152.6(1)
273 K	N1–H1···Br3	0.9798(8)	2.4582(5)	3.3427(1)	150.0(5)
	N1'–H1'···Br3	0.9802(2)	2.3961(5)	3.3220(2)	157.3(1)
293 K	N1–H1···Br3	0.9820(2)	2.4471(6)	3.3346(1)	151.4(6)
	N1'–H1'···Br3	0.9792(1)	2.4389(6)	3.3555(3)	155.1(1)
313 K	N1–H1···Br3	0.9790(1)	2.4267(7)	3.3211(1)	151.7(8)
	N1'–H1'···Br3	0.9789(2)	2.4423(7)	3.3554(3)	155.1(2)

Table S4 The fitted parameters with Debye equation for **1** at 150 ~ 230 K

T (K)	τ_0 (s)	ε_0	ε_∞	$\Delta\varepsilon$
150	1.0×10^{-4}	3.39	3.21	0.18
160	3.9×10^{-5}	3.44	3.23	0.21
170	1.5×10^{-5}	3.48	3.25	0.23
180	7.7×10^{-6}	3.53	3.28	0.25
190	3.5×10^{-6}	3.58	3.30	0.28
200	1.8×10^{-6}	3.62	3.33	0.29
210	1.0×10^{-6}	3.68	3.37	0.31
220	5.4×10^{-7}	3.74	3.41	0.33
230	3.8×10^{-7}	3.81	3.45	0.36

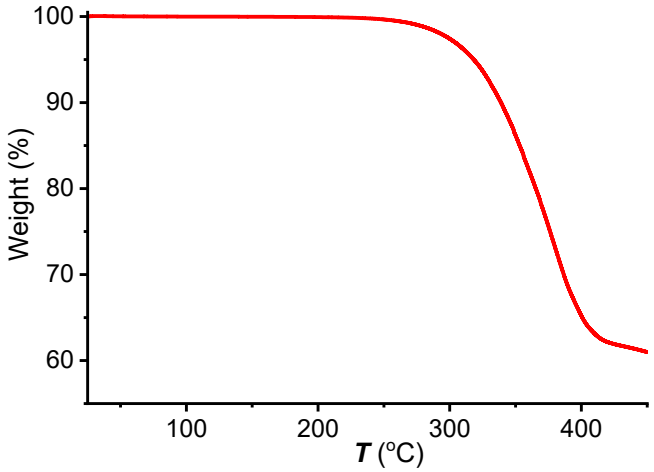

Fig. S1 TGA curve of **1**.

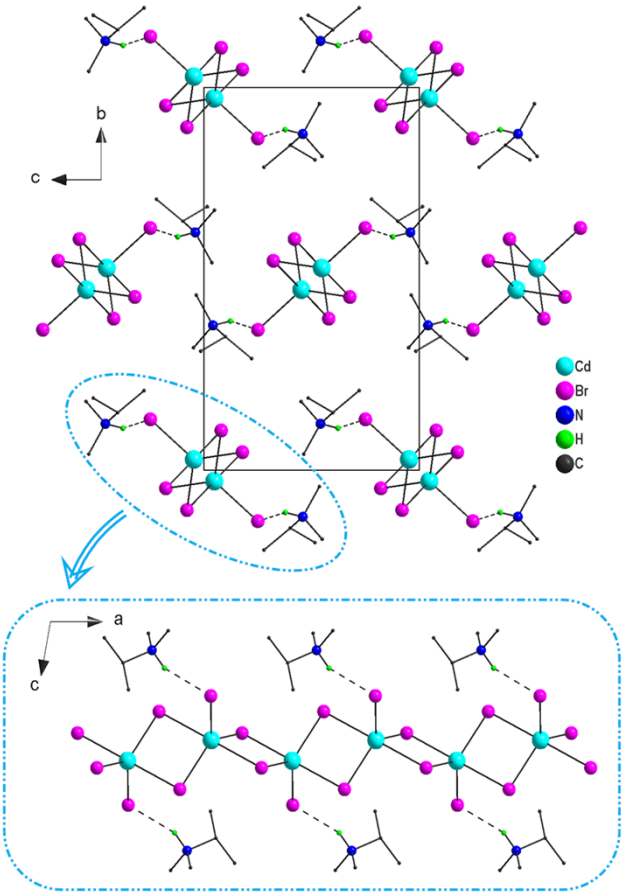

Fig. S2 View of the structure of **1** at 173 K.

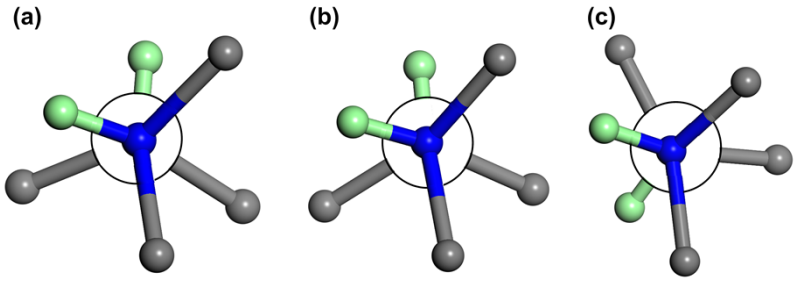

Fig. S3 Newman projections of the N1-containing $(i\text{-PrNHMe}_2)^+$ ion at 173 K (a), 313 K (b), and the N1′-containing one (c) along the N−C bond.

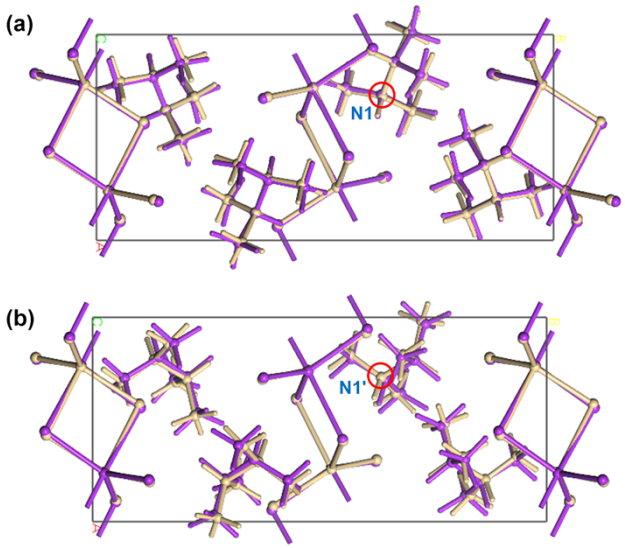

Fig. S4 Overlapping maps of the crystal structures of **1** (at 313 K) before/after geometry optimization (shaded in yellow/purple, respectively), with merely the N1-containing $(i\text{-PrNHMe}_2)^+$ cations (a) or merely the N1'-containing ones (b).

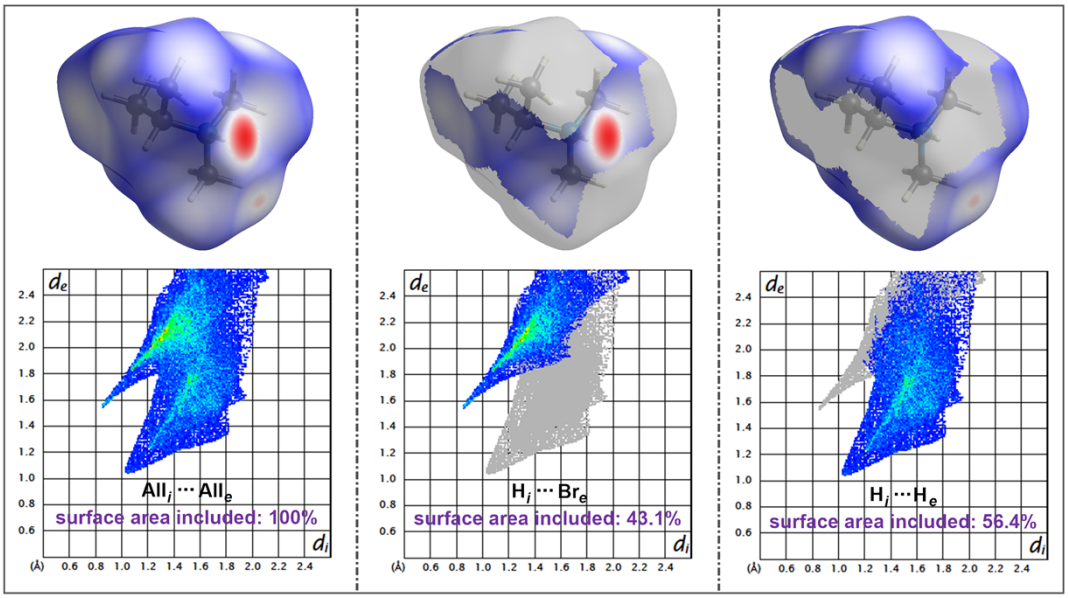

Fig. S5 Above: Views of the Hirshfeld surface (mapped with d_{norm}) of the N1-containing $(i\text{-PrNHMe}_2)^+$ cation in **1** at 313 K, indicating the relative strength of the intermolecular interactions surrounding the $(i\text{-PrNHMe}_2)^+$ cation. The red, white, and blue regions represent molecular contacts shorter than, equal to, and longer than the van der Waals distance, respectively. Below: 2D fingerprint plots showing atomic contacts to the Hirshfeld surface of the N1-containing $(i\text{-PrNHMe}_2)^+$ cation in **1** at 313 K, where d_i and d_e denote the distances from the surface to the nearest atom interior and exterior to the surface, respectively. The 2D plots were created by binning (d_e, d_i) pairs and coloring each bin of the resulting 2D histogram as a function of the fraction of surface points in that bin, ranging from blue (few points) through green to red (many points).

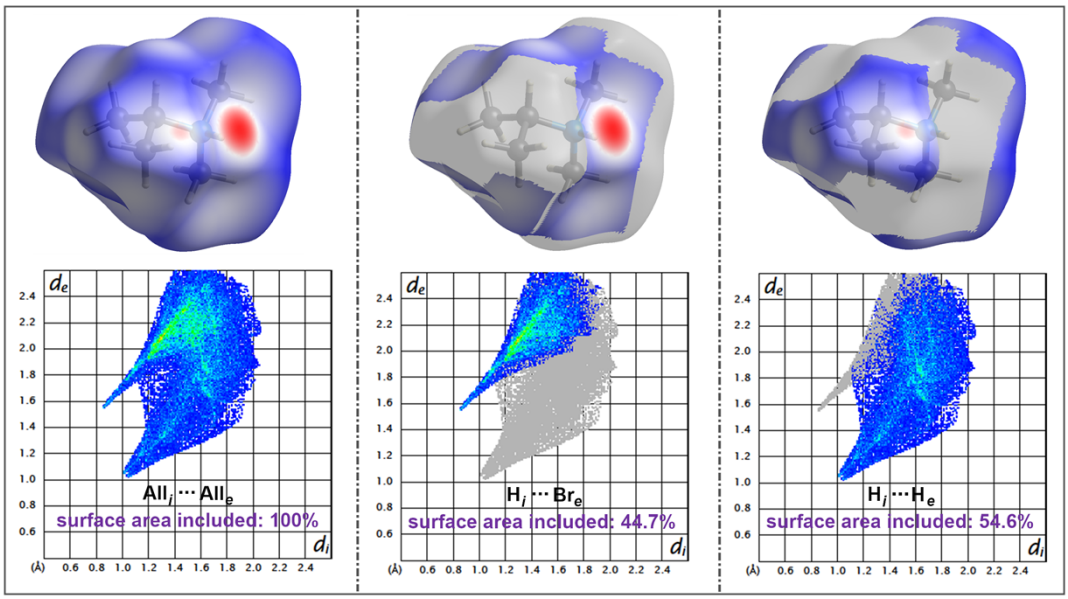

Fig. S6 Above: Views of the Hirshfeld surface (mapped with d_{norm}) of the N1′-containing (*i*-PrNHMe$_2$)$^+$ cation in **1** at 313 K. Below: 2D fingerprint plots showing atomic contacts to the Hirshfeld surface of the N1′-containing (*i*-PrNHMe$_2$)$^+$ cation in **1** at 313 K. For display details, see the figure caption of Fig. S5.

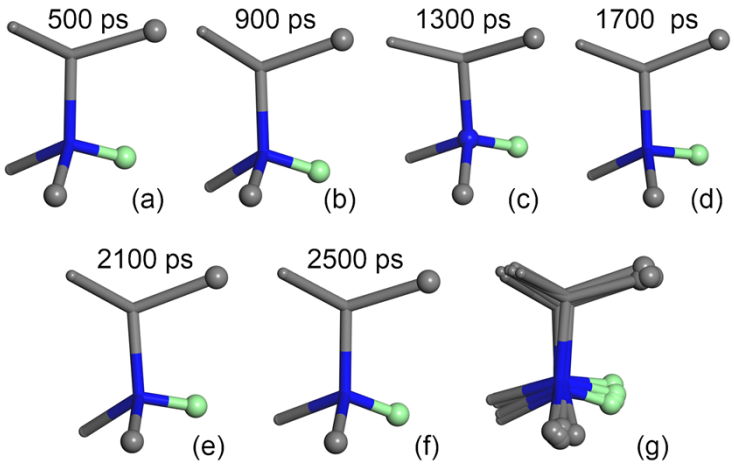

Fig. S7 Snapshots of NVT dynamic simulation for the (*i*-PrNHMe$_2$)$^+$ cation of **1** at T_S of 173 K (a-f), and the overlapping maps of these snapshots (g), to display their dynamics. The specified H and C atoms are highlighted by balls to guide the eye.

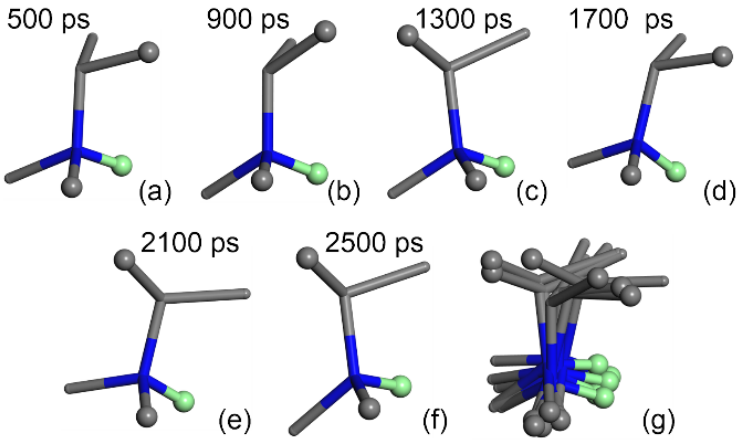

Fig. S8 Snapshots of NVT dynamic simulation for the $(i\text{-PrNHMe}_2)^+$ cation of **1** at T_S of 373 K (a-f), and the overlapping maps of these snapshots (g), to display their dynamics. The specified H and C atoms are highlighted by balls to guide the eye.

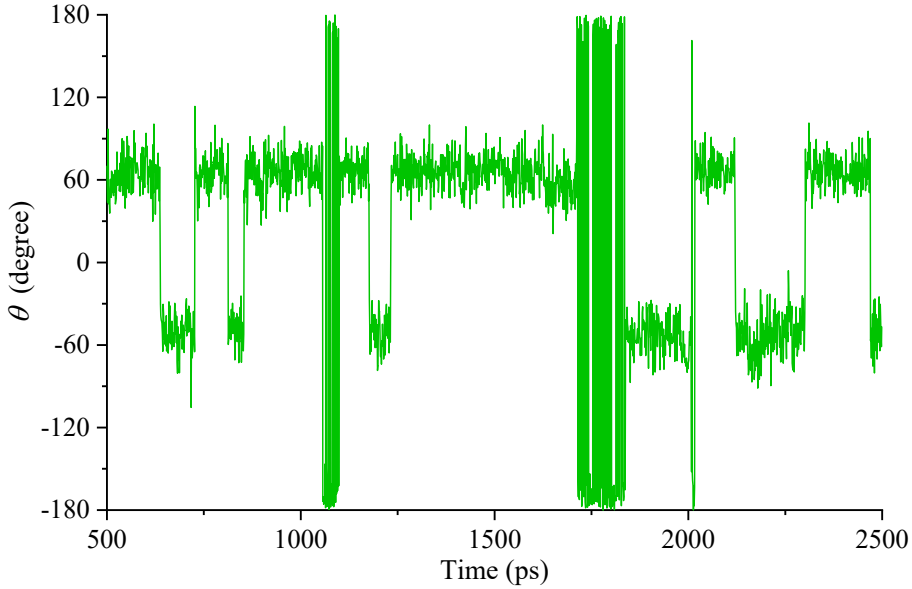

Fig. S9 The evolution of the torsion ϑ over simulation time from 500 to 2500 ps, at T_S of 373 K.

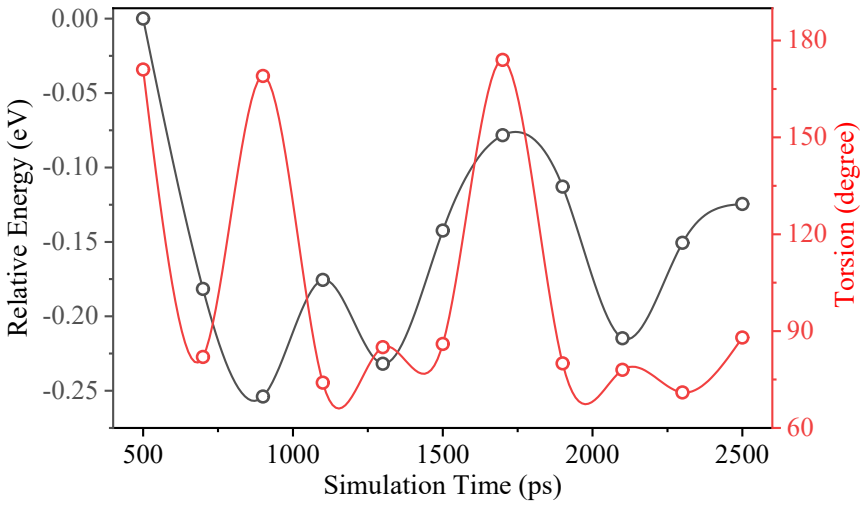

Fig. S10 Variations of the relative potential energy for **1** (based on DFT calculation) and the torsion $\vartheta_{(H-N-C-H)}$ of one selected $(i\text{-PrNHMe}_2)^+$ ion during the MD simulation process (at T_S of 373 K), over the simulation time from 500 to 2500 ps (in an increasing step of 200 ps).

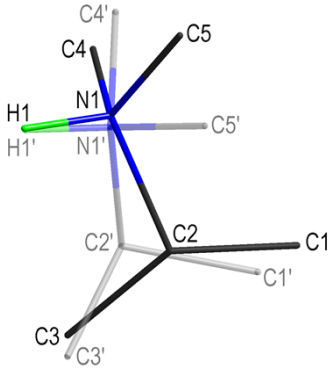

Fig. S11 The two-fold disordered states of the $(i\text{-PrNHMe}_2)^+$ ion in the crystal structure of **1** at 313K.

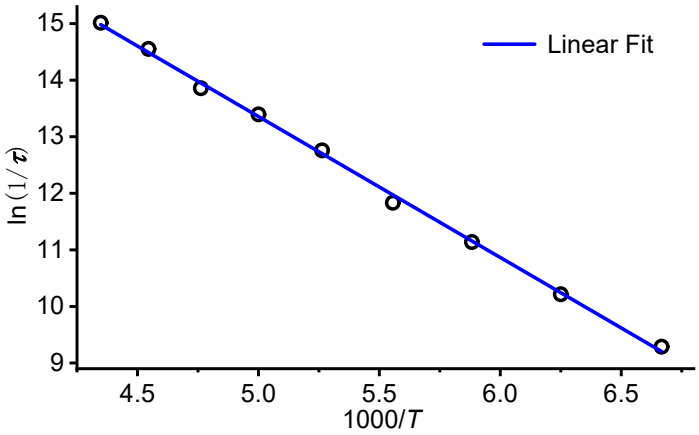

Fig. S12 Arrhenius plot of the relaxation time τ as a function of inverse temperature for a single relaxation process of **1**.

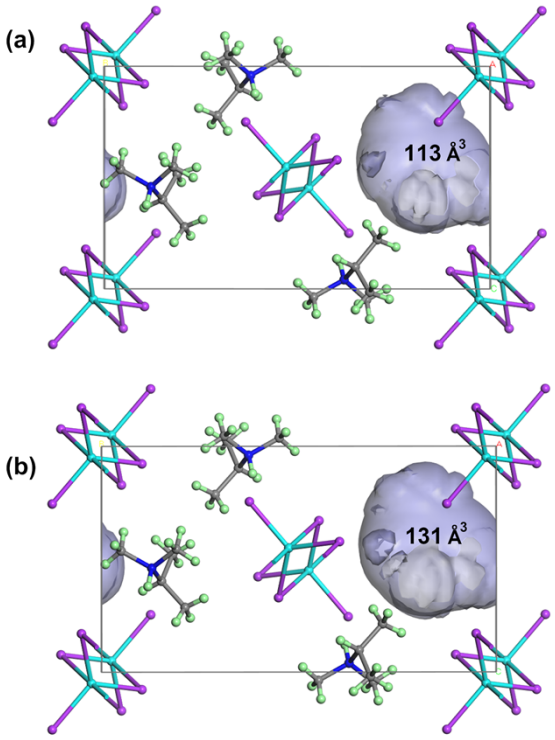

Fig. S13 Variable confined space for the (*i*-PrNHMe$_2$)$^+$ cations at 173 K (a) and 313 K (b), respectively. Cd, N, C, and H atoms are shaded in cyan, blue, grey, and green, respectively.

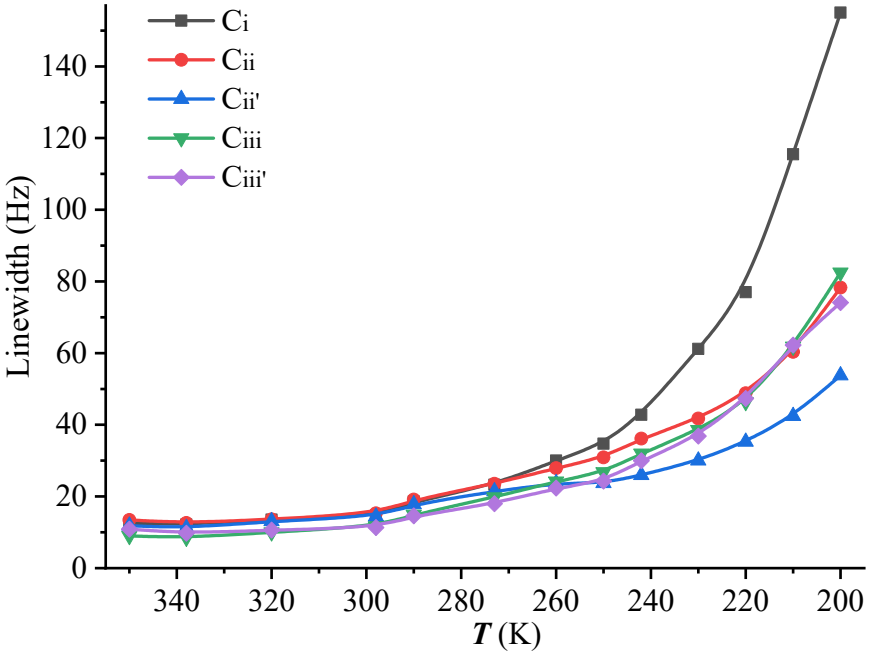

Fig. S14 Temperature-dependent linewidth for the (*i*-PrNHMe$_2$)$^+$ ion in **1**.

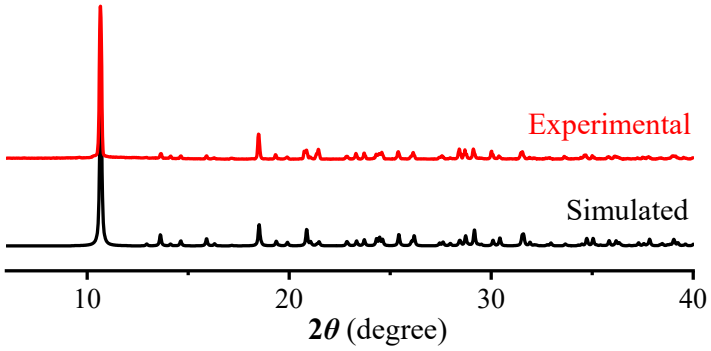

Fig. S15 Simulated and experimental PXRD patterns for **1** at 293 K.